Dalton Transactions

Accepted Manuscript

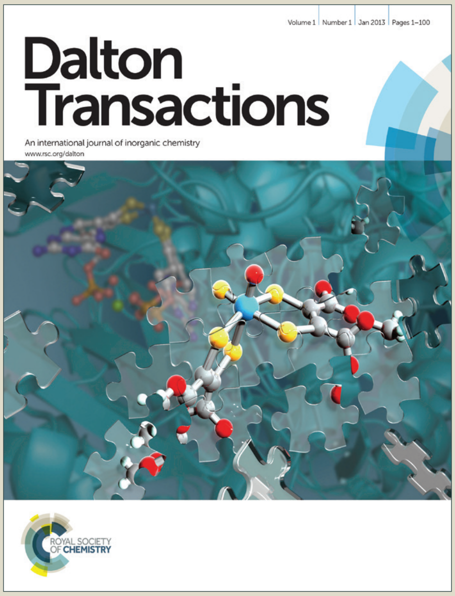

Dalton Transactions RSCPublishing

ARTICLE

Cite this: DOI: 10.1039/x0xx00000x

Received 00th January 2012,
Accepted 00th January 2012

DOI: 10.1039/x0xx00000x

www.rsc.org/

Variation of Electronic Transitions and Reduction Potentials of Cerium(IV) Complexes

Ursula J. Williams,[a] David Schneider,[b] Walter L. Dorfner,[a] Cäcilia Maichle-Mössmer,[b] Patrick J. Carroll,[a] Reiner Anwander*[b] and Eric J. Schelter*[a]

The trivalent compound K[Ce[N(SiHMe$_2$)$_2$]$_4$] was synthesized and oxidized, providing a convenient route to the reported cerium(IV) compound, Ce[N(SiHMe$_2$)$_2$]$_4$. Protonolysis reactions of Ce[N(SiHMe$_2$)$_2$]$_4$ with *tert*-butanol, substituted benzyl alcohols, and 2,6-diphenylphenol yielded the neutral tetravalent compounds Ce(O^{t}Bu)$_4$(py)$_2$, Ce$_2$(OCH$_2$C$_6$R$_5$)$_8$(thf)$_2$ (R = Me, F), and Ce(Odpp)$_4$ (dpp = C$_6$H$_3$-2,6-(C$_6$H$_5$)$_2$). Spectroscopic and electrochemical characterization of the mononuclear cerium(IV) silylamide, alkoxide, and aryloxide compounds revealed variable ligand-to-metal charge transfer transitions and metal-based reduction potentials. Computational bonding analysis was performed to complement the physical characterization of the complexes.

Introduction

Recent research efforts in the molecular chemistry of cerium have sought to understand and control the redox behavior of the element and to stabilize its tetravalent oxidation state.[1-10] Synthetic strategies that have been developed to access homoleptic cerium(IV) coordination compounds include oxidation of related cerium(III) starting materials, often involving ligand redistribution,[4, 11-13] and metathesis reactions using alkoxide, nitrate, or mixed alkoxide/nitrate starting materials.[14-17] In a few examples, protonolysis of cerium(IV) alkoxide starting materials was used to isolate cerium(IV) containing products.[18, 19]

The homoleptic cerium(IV) silylamide compound Ce[N(SiHMe$_2$)$_2$]$_4$ was recently reported from oxidation of Ce[N(SiHMe$_2$)$_2$]$_3$(THF)$_2$ or Li(THF)[Ce(N(SiHMe$_2$)$_2$)$_4$].[13, 20] Trivalent lanthanide complexes of the bis(dimethylsilyl)amide ligand have been shown to readily undergo protonolysis reactions with alcohols and phenols.[21-27] In one reported example, Ce[N(SiHMe$_2$)$_2$]$_4$ underwent protonolysis to provide cerium(IV) formamidinate complexes.[20] In this context, we were interested in expanding the protonolysis chemistry of Ce[N(SiHMe$_2$)$_2$]$_4$ in order to isolate cerium(IV) complexes with alkoxide and aryloxide ligand frameworks.

A growing body of work has demonstrated that, despite the ionic nature of lanthanide-ligand bonding, the ligand environment of the cerium cation significantly impacts its physicochemical properties. Such effects have been noted in the tunability of the cerium(III/IV) electrochemical couple.[28] Reported cerium(III/IV) redox couples span an electrochemical range of greater than 3 V, from aqueous acidic conditions (+1.63 V vs SCE; Ce(ClO$_4$)$_3$ in 8 M HClO$_4$) to nonaqueous conditions in a pyridylnitroxide ligand field (–1.49 V vs SCE; Ce(2-^{t}BuNO-py)$_4$ in dichloromethane).[4, 29] A second characteristic of cerium(IV) coordination compounds is the intense ligand-to-metal charge transfer (LMCT) in the UV and visible ranges of their electronic absorption spectra.[4, 6-9, 30, 31] These transitions typically result in intensely colored cerium(IV) compounds. The energies of these LMCT bands are reportedly highly variable among cerium(IV) coordination compounds,[4, 6-9, 30, 31] but little has been done to systematically explore the effect of ligand environments on the spectroscopic characteristics of the resulting compounds.

We set out to synthesize and characterize neutral cerium(IV) compounds using monodentate monoanionic ligands to assess the effect of ligand fields on the metal-based reduction potentials and charge transfer transitions. Here we report a rational synthesis of Ce[N(SiHMe$_2$)$_2$]$_4$ through oxidation of the trivalent compound K[Ce[N(SiHMe$_2$)$_2$]$_4$. The capability of Ce[N(SiHMe$_2$)$_2$]$_4$ to act as a protonolysis precursor is shown for several alcohol and phenol substrates, leading to the isolation of mono- and dinuclear tetrakis(alkoxide) and tetrakis(aryloxide) cerium(IV) compounds. The spectroscopic, electrochemical, and computational analyses of the mononuclear cerium(IV) complexes studied here provide a comparison of the effect of amide, alkoxide, and aryloxide coordination on the properties of cerium(IV) coordination compounds.

Experimental

Methods. All reactions and manipulations were performed under an inert atmosphere (N$_2$ or Ar) using standard Schlenk techniques or in a Vacuum Atmospheres, Inc. Nexus II drybox equipped with a molecular sieves 13X / Q5 Cu–0226S catalyst purifier system or a MBraun MB150B-G-II glovebox (< 0.1

ppm H_2O, O_2). Glassware was oven-dried for 3 hours at 150 °C prior to use. ^1H NMR and ^{13}C NMR spectra were obtained on a Bruker DMX–300 Fourier transform NMR spectrometer at 300 MHz and 91 MHz as well as on Bruker AVII+400 or AVII+500 NMR spectrometers using deuterated, dry solvents. Chemical shifts were recorded in units of parts per million referenced to residual solvent peaks (^1H) or characteristic solvent peaks ($^{13}C\{^1H\}$). The UV-Visible absorption spectra were obtained from 1000–300 nm using a Perkin Elmer 950 UV-Vis/NIR Spectrophotometer, and all samples were prepared under an N_2 environment. Air tight, screw cap quartz cells of 1 mm pathlength were used with a blank measured before each run. Deconvolution of the UV-Vis spectra was performed using fityk.[32] Elemental analyses were performed at the University of California, Berkeley Microanalytical Facility using a Perkin-Elmer Series II 2400 CHNS analyzer and at the University of Tübingen using an Elementar vario MICRO cube.

Electrochemistry. Cyclic voltammetry experiments were performed using a CH Instruments 620D Electrochemical Analyzer/Workstation and the data were processed using CHI software v 9.24. All experiments were performed in an N_2 atmosphere drybox using electrochemical cells that consisted of a 4 mL vial, a glassy carbon (2 mm diameter) working electrode, a platinum wire counter electrode, and a silver wire plated with AgCl as a quasi-reference electrode. The working electrode surfaces were polished prior to each set of experiments. Potentials were reported versus ferrocene, which was added as an internal standard for calibration at the end of each run. Solutions employed during CV studies were ~1 mM in analyte and 100 mM in $[^nPr_4N][B(3,5\text{-}(CF_3)_2\text{-}C_6H_3)_4]$ ($[^nPr_4N][BAr^F{}_4]$). All data were collected in a positive-feedback IR compensation mode. The solution cell resistances were measured prior to each run to ensure resistances ≤ ~500 Ω.

X-ray Crystallography. X-ray intensity data for compounds **2**, **4**, **5**, **6**, and **7** were collected on a Bruker APEXII CCD area detector employing graphite-monochromated Mo-Kα radiation (λ=0.71073 Å) at temperatures of 143(1), 143(1), 100(1), 100(2), or 293(2) K, respectively. Data collection and reduction were done using the Bruker AXS APEX2 program package.[33] Structure solution and refinement were accomplished using the programs SHELXS and SHELXL, respectively.[34]

Computational Details. Gaussian '09 Rev. A.02 was used in electronic structure calculations.[35] The B3LYP hybrid DFT method was employed with a 28-electron small core pseudopotential on cerium with published segmented natural orbital basis sets incorporating quasi-relativistic effects[36] and the 6-31G* basis set on all other atoms. Gas phase geometry optimizations were carried out starting from the coordinates of the crystal structures. The frequency calculations indicated that the geometries were the minima (no imaginary frequencies). Molecular orbitals were rendered with the program Chemcraft v1.6 at an isovalue of 0.03.[37] Natural population analysis was performed using the IOp(6/80=1) keyword in Gaussian '09.

Materials. THF, hexanes, *n*-hexane, diethyl ether, toluene, *n*-pentane, and dichloromethane were purchased from Fisher Scientific. These solvents were sparged for 20 min with dry argon and dried using a commercial solvent purification system comprising two columns packed with Q5 reactant and neutral alumina respectively, or using Grubbs columns (MBraun, Solvent Purification System). $HN(SiHMe_2)_2$ (Alfa Aesar), Ph_3CCl (Acros Organics), 2,6-diphenylphenol (Acros Organics), pentamethyl benzyl alcohol (Sigma Aldrich) and pentafluoro benzyl alcohol (Sigma Aldrich) were purchased and used as received. Ferrocene (Fc) was purchased from Acros Organics and purified by sublimation before use. Benzene-*d₆*, toluene-*d₈*, and THF-*d₈* were purchased from Cambridge Isotopes and dried over potassium mirror for 24 h before use. Pyridine-*d₅* was purchased from Cambridge Isotopes and dried over 4 Å molecular sieves for 24 h before use. *Tert*-butanol was purchased from Fisher Scientific, degassed, and dried over 4 Å molecular sieves before use. $Ce[N(SiMe_3)_2]_3$,[38] $Ce[N(SiHMe_2)_2]_3(THF)_2$,[39, 40] $KN(SiHMe_2)_2$,[41] and $[^nPr_4N][BAr^F{}_4]$[42] were prepared according to published procedures.

Synthesis of $K[Ce[N(SiHMe_2)_2]_4]$, (2). $KN(SiHMe_2)_2$ (0.38 g, 1.91 mmol) was added to a stirred solution of 1.31 g (1.92 mmol) $Ce[N(SiHMe_2)_2]_3(THF)_2$ in ~10 mL hexanes. After 5 h, a colorless precipitate was isolated over a medium porosity fritted filter, washed 2 × 3 mL hexanes, and dried under reduced pressure to isolate the product as a colorless powder. Yield: 1.04 g (1.46 mmol, 77%) Light yellow X-ray diffraction quality crystals were isolated from slow evaporation of a hexanes/diethyl ether solution (3:1) at room temperature. Anal. Calcd. for $KCeC_{16}H_{56}N_4Si_8$: C, 27.12; H, 7.97; N, 7.91. Found: C, 27.07; H, 7.61; N, 7.86. ^1H NMR (pyridine-*d₅*): δ 1.61 (s, 48H, CH_3), –8.27 (broad s, 8H, Si*H*).

Preparative Scale Synthesis of $Ce[N(SiHMe_2)_2]_4$, (3). Ph_3CCl (0.169 g, 0.606 mmol) was added to a stirred solution of 0.426 g (0.601 mmol) $K[Ce[N(SiHMe_2)_2]_4]$ in ~10 mL THF, inducing a color change to dark red. After 1 h, the reaction was dried under reduced pressure and the product was extracted using ~10 mL hexanes. The reaction was filtered through a Celite-packed, coarse porosity fritted filter and concentrated to a volume of ~5 mL. The concentrated hexanes solution was chilled at –35 °C overnight, inducing precipitation of the organic byproduct. The reaction was filtered through a Celite-packed coarse porosity fritted filter to remove the organic product. The filtrate, a pure solution of $Ce[N(SiHMe_2)_2]_4$, was dried under reduced pressure to isolate the product as a dark red microcrystalline solid. Yield: 0.257 g (0.384 mmol, 64%) Anal. Calcd. for $CeC_{16}H_{56}N_4Si_8$: C, 28.70; H, 8.43; N, 8.37. Found: C, 28.42; H, 8.45; N, 8.02. ^1H NMR (C_6D_6): δ 6.01 (m, 8H, Si*H*), 0.35 (d, 48H, CH_3). ^{13}C NMR (C_6D_6): δ 2.28 ($SiCH_3$).

NMR Scale Synthesis of $Ce[N[SiHMe_2]_2]_4$ in Tol-*d₈*. $K[Ce[N(SiHMe_2)_2]_4]$ (0.0419 g, 0.0591 mmol) was suspended in 1.5 mL toluene-*d₈* in a J. Young valve NMR tube. Ph_3CCl (0.0165 g, 0.0591 mmol) was added and the tube was sealed and shaken, then left to stand for 2 h at room temperature. Ferrocene (0.0110 g, 0.0591 mmol) was added to the red solution and resealed. Integration of the ferrocene standard to the product peak in the ^1H NMR spectrum indicated 99% conversion.

NMR Scale Synthesis of $Ce[N[SiHMe_2]_2]_4$ in THF-*d₈*. $K[Ce[N(SiHMe_2)_2]_4]$ (0.0419 g, 0.0591 mmol) was dissolved in 1.5 mL THF-*d₈* in a J. Young valve NMR tube. Ph_3CCl (0.0165 g, 0.0591 mmol) was added, the tube was sealed and shaken, then left to stand for 2 h at room temperature. Ferrocene (0.0110 g, 0.0591 mmol) was added to the red solution and resealed. Integration of the ferrocene standard to the product peak in the ^1H NMR spectrum indicated quantitative conversion.

Synthesis of $Ce(O^tBu)_4(py)_2$, (4). A solution of $Ce[N(SiHMe_2)_2]_4$ (0.114 g, 0.170 mmol) dissolved in ~5 mL hexanes was added slowly to a solution of 0.073 g (0.99 mmol) *tert*-butanol dissolved in ~5 mL hexanes. 5 drops of pyridine were added, and the solution was mixed for 1 min. Volatiles were removed under reduced pressure. The resultant yellow solid was redissolved in ~1 mL hexanes with 1 drop of pyridine and chilled at –35 °C. The crystals that precipitated from the solution were shown to have the formula $Ce(O^tBu)_4(py)_2$ by X-ray diffraction. To collect preparative amounts of pure compound, the mother liquor was removed by decantation, and the crystals were dried briefly under reduced pressure, then left under ambient drybox atmosphere for 2 h. Following these purification steps, the product was shown to have the formula $Ce(O^tBu)_4(py)_{1.5}$ by ^1H NMR and combustion analysis. Yield: 0.063 g (0.14 mmol, 67%) Anal. Calcd. for $CeC_{23.5}H_{43.5}N_{1.5}O_4$: C, 51.2; H, 7.95; N, 3.81. Found: C, 51.0; H, 7.59; N, 4.21. ^1H NMR (C_6D_6): δ 8.69 (broad s, 6H, Ar-*H*), 6.94 (t, 3H, 7.7 Hz, Ar-*H*), 6.68 (t, 6.6 Hz, 6H, Ar-*H*), 1.63 (s, 72H, C(C*H*$_3$)$_3$). ^{13}C NMR (C_6D_6): δ 150.72 (N*C*$_5$H$_5$), 136.00 (N*C*$_5$H$_5$), 123.49 (N*C*$_5$H$_5$), 81.03 (O*C*(CH$_3$)$_3$), 34.55 (OC(*C*H$_3$)$_3$).

Synthesis of Ce(Odpp)$_4$ (dpp = C_6H_3-2,6-(C_6H_5)$_2$) (5). $Ce[N(SiHMe_2)_2]_4$ (0.134 g, 0.200 mmol) was dissolved in ~3 mL toluene. 2,6-diphenylphenol (0.197 g, 0.801 mmol) was added with stirring. After 30 min, the resultant dark blue solution was dried under reduced pressure. The solid was suspended in ~10 mL hexanes, collected over a medium porosity fritted filter, washed with 1 × 10 mL hexanes and dried under reduced pressure to isolate the product as a blue powder. Yield: 0.174 g (0.156 mmol, 78%). Dark blue X-ray diffraction quality crystals were isolated from a concentrated toluene solution at –35 °C. Anal. Calcd. for $CeC_{72}H_{52}O_4$: C, 77.12; H, 4.67. Found: C, 77.25; H, 4.86; N, < 0.2. ^1H NMR (C_6D_6): δ 7.22 (d, 7.2 Hz, 16H, OC$_6$H$_3$(C$_6$*H*$_5$)$_2$), 7.12 (d, 7.5 Hz, 8H, O*C*$_6$H$_3$Ph$_2$), 6.93 (t, 16H, 7.5 Hz, OC$_6$H$_3$(C$_6$*H*$_5$)$_2$), 6.80 (tt, 7.4, 1.5 Hz, 8H, OC$_6$H$_3$(C$_6$*H*$_5$)$_2$), 6.61 (t, 7.5 Hz, 4H, OC$_6$*H*$_3$Ph$_2$). ^{13}C NMR (C_6D_6): δ 166.32 (O*C*$_6$H$_3$Ph$_2$), 140.64 (OC$_6$H$_3$(*C*$_6$H$_5$)$_2$), 132.72 (OC$_6$H$_3$(*C*$_6$H$_5$)$_2$), 129.60 (OC$_6$H$_3$(*C*$_6$H$_5$)$_2$), 129.41 (OC$_6$H$_3$(*C*$_6$H$_5$)$_2$), 129.21 (O*C*$_6$H$_3$Ph$_2$), 127.30 (O*C*$_6$H$_3$Ph$_2$), 121.83 (O*C*$_6$H$_3$Ph$_2$).

Synthesis of Ce$_2$(OCH$_2$C$_6$Me$_5$)$_8$(THF)$_2$ (6). $Ce[N(SiHMe_2)_2]_4$ (0.107 g, 0.160 mmol) was dissolved in ~2 mL THF and added dropwise to a solution of 0.138 g (0.774 mmol) $HOCH_2C_6Me_5$ in THF (~3 mL). Instantaneous reaction was indicated by a color change of the initially red solution to yellow. After stirring the reaction for 30 min at ambient temperature, all volatiles were removed under reduced pressure and the remaining yellow powder was crystallized from a concentrated THF/*n*-hexane solution (3:1). Yield: 0.124 g (0.067 mmol, 84%) X-ray diffraction quality crystals were isolated from a concentrated benzene-*d$_6$* solution. Anal. Calcd. for $Ce_2C_{104}H_{152}O_{10}$: C, 67.8; H, 8.31; N, 0.0; Found: C, 67.45; H, 7.94; N: 0.05. ^1H NMR (toluene-*d$_8$*): δ 5.58 (s, 8H, C*H*$_2$), 3.46 (C*H*$_2$-THF), 2.54 (s, 24H, Ar-*o*C*H*$_3$) 2.08–2.07 (2 s, 36 H, Ar-C*H*$_3$), 1.32 (C*H*$_2$-THF). ^{13}C NMR (toluene-*d$_8$*): δ 138.0 (*C*-Ar), 133.3 (*C*-Ar), 133.0 (*C*-Ar), 131.8 (*C*-Ar), 73.1 (*C*H$_2$) 68.4 (O*C*H$_2$-THF), 25.7 (*C*H$_2$-THF), 16.9 (Ar-*Me*), 16.7 (Ar*Me*, overlapping features).

Synthesis of Ce$_2$(OCH$_2$C$_6$F$_5$)$_8$(THF)$_2$ (7). $Ce[N(SiHMe_2)_2]_4$ (0.128 g, 0.191 mmol) was dissolved in ~5 mL THF and added dropwise to a solution of 0.181 g (0.914 mmol) $HOCH_2C_6F_5$ in ~5 mL THF. The reaction mixture turned yellow immediately and was stirred at ambient temperature for 10 min. Then the mixture was dried under reduced pressure leaving a yellow powder, which was crystallized from a concentrated THF solution. Yield: 0.164 g (0.082 mmol, 86%) Anal. Calcd. for $Ce_2C_{64}H_{32}F_{40}O_{10}$: C, 38.4; H, 1.61. Found: C, 38.2; H, 1.15. ^1H NMR (benzene-*d$_6$*): δ 3.50 (s, *THF*), 1.68 (s, *THF*), 1.27 (s, O-C*H$_2$*); ^{19}F NMR (benzene-*d$_6$*): δ -162.48 (s, 8F, *o-F*), -167.74 (t, 19 Hz, 8F, *m-F*), -180.41 (t, 19 Hz, 4F, *p-F*); ^{13}C NMR (benzene-*d$_6$*): δ 67.6 (O-THF), 64.9 (C*H$_2$*-O), 25.8 (THF) (ring-carbon atoms could not be clearly detected).

Results and Discussion

Synthesis and structural characterization

The trivalent compounds of the bis(dimethylsilyl)amide ligand, $Ln[N(SiHMe_2)_3](THF)_2$ (Ln = La, Ce (**1**), Pr, Nd, Sm, Eu, Gd, Ho, Er, Yb, Lu), were reported from metathesis of $LnCl_3(THF)_2$ and by protonolysis of the bis(trimethylsilyl)amide precursors, $Ln[N(SiMe_3)_2]_3$.[13, 39, 40, 43-47] The solid-state structure of compound **1** was shown recently to be isomorphous with the reported lanthanum(III) analogue.[39, 48] Addition of $KN(SiHMe_2)_2$ to a hexanes solution of compound **1** led to coordination of a fourth silylamide equivalent to the cerium(III) ion and induced precipitation of the cerium(III)-containing compound $K[Ce[N(SiHMe_2)_2]_4]$ (**2**) (Scheme 1).[20, 49]

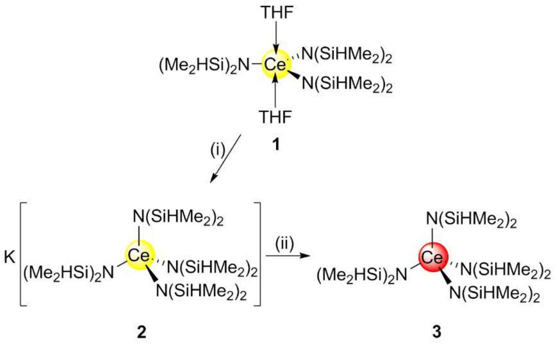

Scheme 1. Synthesis of compounds **1**, **2**, and **3**. (i) $KN(SiMe_2)_2$, hexanes, 5 h. (ii) Ph_3CCl, THF, 1 h.

The crystal structure of **2** is shown in Figure 1. Compound **2** crystallized as a solvent-free coordination polymer in the monoclinic C2/c space group. The symmetry about the cerium ion was pseudo-tetrahedral, with a τ_4 parameter of 0.88.[50] The Ce–N bond distances in the compound of 2.3820(12) and 2.4379(12) Å were similar to the Ce–N bond distances in compound **1**.[48] Two of the eight silyl protons in the molecular unit showed short contacts to the Ce(III) center, with SiH→Ce distances of 2.81(2) Å (Si–H = 1.423(17) Å), and Ce–Si distances of 3.2711(4) Å. The remaining silyl protons were detected in close contact with the unsolvated potassium ions in the lattice. A related complex, $\{Li[Y[N(SiHMe_2)_2]_4]\}_2$, has been reported and was synthesized from metathesis of $Y(OTf)_3$ (OTf = $CF_3SO_3^-$) with 4 equiv $LiN(SiHMe_2)_2$ and similarly contained intermolecular SiH→Li interactions in the dimeric structure.[51]

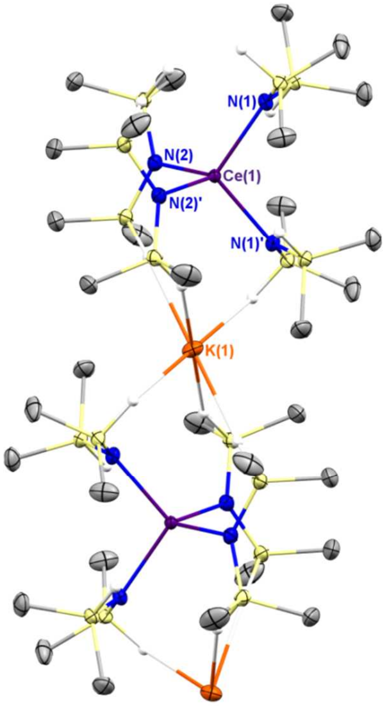

Figure 1. 30% probability thermal ellipsoid plot of compound **2** showing the polymeric structure. Methyl hydrogen atoms have been omitted for clarity. Selected bond distances: Ce(1)–N(1): 2.4379(12) Å, Ce(1)–N(2): 2.3820(12) Å.

Compound **2** was insoluble in non-coordinating solvents including benzene, toluene, hexanes and *n*-pentane, but was soluble in the coordinating solvents Et_2O, THF, and pyridine. In pyridine-d_5 **2** exhibited broad singlets in its ^{1}H NMR spectrum at –1.61 and –8.27 ppm which corresponded to 48 methyl and 8 silyl protons respectively. THF solutions of compound **2** underwent complete desolvation upon application of vacuum, as evidenced by a lack of THF resonances in the ^{1}H NMR subsequently recorded in pyridine-d_5.

Upon oxidation of **2** with Ph_3CCl, a color change to dark red was observed. The reaction product was identified as the previously reported tetravalent compound $Ce[N(SiHMe_2)_2]_4$ (**3**).[13] Notably, oxidation of **2** was insensitive to the choice of coordinating or noncoordinating solvent, in contrast to reported syntheses of **3** from oxidation of $Ce[N(SiHMe_2)_2]_3(THF)_x$ (x = 0, 2) or $Li(THF)[Ce[N(SiHMe_2)_2]_4]$.[13, 20] Reactions of **2** with Ph_3CCl in toluene-d_8 and THF-d_8 monitored with a ferrocene internal standard showed quantitative conversion to **3** in 2 h.

To probe whether the alcoholysis observed for bis(dimethylsilyl)amide complexes of rare earth metals could be extended to homoleptic tetravalent compound **3**,[21-27] we examined the reactivity of **3** with a variety of alcohols and phenols (Scheme 2). Upon reaction of **3** with excess *tert*-butanol in hexanes, a fast color change from dark red to yellow was observed. A yellow crystalline solid was isolated following exposure to pyridine and crystallization from a concentrated hexanes solution at –35 °C. X-ray crystallographic characterization showed that the reaction product had formed by complete protonolysis to yield the recently reported compound $Ce(O^tBu)_4(py)_2$ (**4**).[52] Isolation of this compound was previously reported from metathesis of $(NH_4)_2Ce(NO_3)_6$ with KO^tBu or NaO^tBu in THF followed by solvent substitution.[15, 52] Crystals isolated by our method showed distinct crystal morphology compared to previously reported data, which prompted us to include structural analysis of **4** (Table S1 and Figure S1).[52] Compound **4** crystallized in the monoclinic C2/c space group. The Ce–O bond distances of 2.0897(13) and 2.1203(12) Å and the Ce–N distances of 2.6733(14) Å were consistent within error to the bond distances in the previously reported conformer of **4**.[52] Compound **4** was isomorphous with the reported thorium analogue, $Th(O^tBu)_4(py)_2$.[53] In addition to $Ce(O^tBu)_4(THF)_2$ and $Ce(O^tBu)_4(py)_2$, previously reported mononuclear neutral cerium(IV) alkoxide complexes include $Ce(hfip)_4(donor)$ (hfip = $(CF_3)_2CHOH$, donor = TMEDA, diglyme),[54] and $Ce(OCMe_2{}^iPr)_4(DMAP)$.[55]

Compound **3** likewise underwent protonolysis with 4 equiv of 2,6-diphenylphenol, resulting in a color change from dark red to dark blue. X-ray diffraction analysis of crystals grown from a concentrated toluene solution confirmed that the product was the homoleptic monomeric cerium(IV) aryloxide complex, $Ce(Odpp)_4$ (dpp = C_6H_3-2,6-$(C_6H_5)_2$) (**5**). Compound **5** crystallized in the orthorhombic Pcba space group with two molecules in the asymmetric unit and Ce–O bond distances ranging from 2.101(3) to 2.125(3) Å. Each aryloxide ring was aligned parallel but slipped from a phenyl substituent of a neighboring ligand, indicating arene-arene interactions (Figure S2). The distances between least square planes formed by the interacting aryl rings ranged from 3.360(6)–3.657(6) Å. Trivalent rare earth metal centers coordinated by four 2,6-diphenylphenolate ligands were previously observed in the solid-state structures of charge-separated $[M^I(donor)_n]^+[Ln^{III}(Odpp)_4]^-$ (donor = diglyme, DME) and $[Ln/Ae^{II}(Odpp)_3]^+[Ln^{III}(Odpp)_4]^-$ (Ae = Ca, Sr, Ba)[56-59] or aryloxide-bridged $[M^ILn^{III}(Odpp)_4]$ (M = alkali metal).[60, 61]

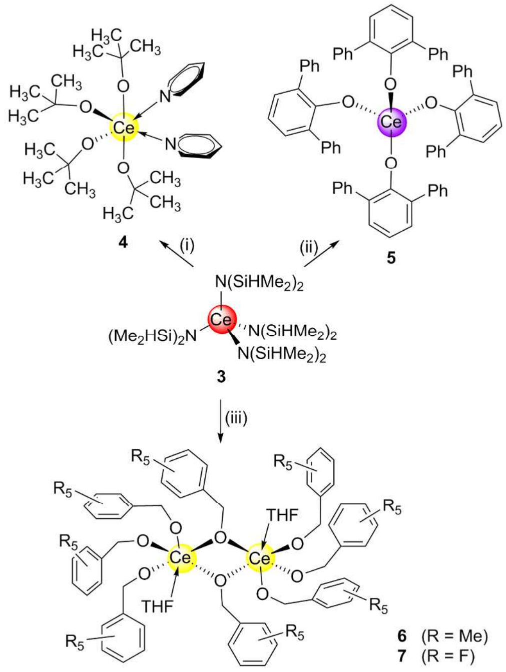

Scheme 2. Synthesis of compounds **4**, **5**, **6**, and **7:** (i) *t*BuOH, hexanes, 5 drops of pyridine, 1 min. (ii) HOdpp, toluene, 30 min. (iii) $HOCH_2Ar$ (Ar = C_6Me_5, C_6F_5), THF, 30/10 min.

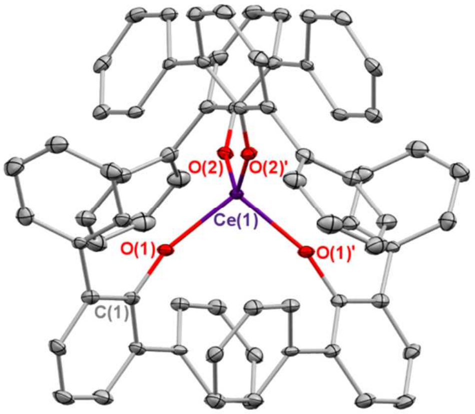

Figure 2. 30% probability thermal ellipsoid plot of compound **5**. Hydrogen atoms have been omitted for clarity. Selected bond distances in **5**: Ce(1)–O(1): 2.101(3) Å, Ce(1)–O(2): 2.125(3) Å, O(1)–C(1): 1.357(6) Å.

Cerium(IV) alkoxides with less sterically demanding ligands were also isolated using pentamethyl and pentafluoro benzyl alcohol in silylamine elimation reactions (Scheme 2).[49] Benzyl alcohol derivatives are scarce in lanthanide and actinide literature. The only lanthanide(III) examples known are heteroleptic complexes with unsubstituted benzyloxy ligands, including the dimeric complexes $\{(MBMP)Ln(\mu_2\text{-}OCH_2Ph)(thf)_2\}_2$ (Ln = Nd, Yb; $MBMP^{2-}$ = 2,2'-methylenebis(6-*tert*-butyl-4-methylphenoxo)), obtained through a protonolysis reaction of $LnCp_3$ with two equivalents of $HOCH_2Ph$ and one equivalent of H_2MBMP,[62] as well as the salalen complexes $[Ln(salalen)(\mu_2\text{-}OCH_2Ph)]_2$ (Ln = Y, Sm, Yb; salalen = $(2\text{-}O\text{-}C_6H_2\text{-}{}^tBu_2\text{-}3,5)CH{=}NCH_2CH_2NMeCH_2\{2\text{-}O\text{-}C_6H_2\text{-}(CPhMe_2)_2\text{-}3,5\}$), obtained either by cyclopentadiene or silylamine elimination.[63] The monomeric amine-bridged bis(phenolate) complex $\{(Me_2NCH_2CH_2N[CH_2\text{-}(2\text{-}OC_6H_2tBu_2\text{-}3,5)]_2\}Y(OCH_2Ph)(thf)$ includes a rare terminal benzyloxy ligand.[64]

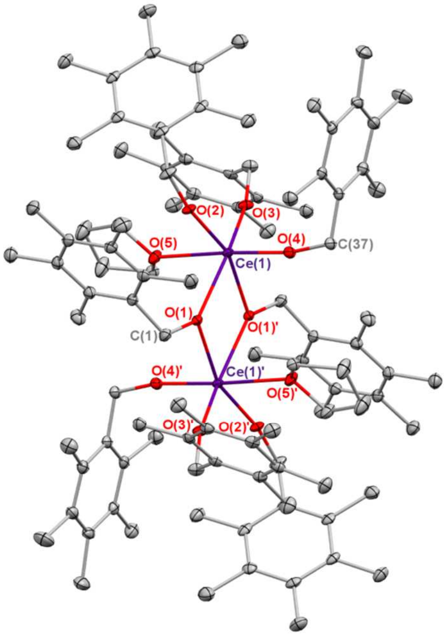

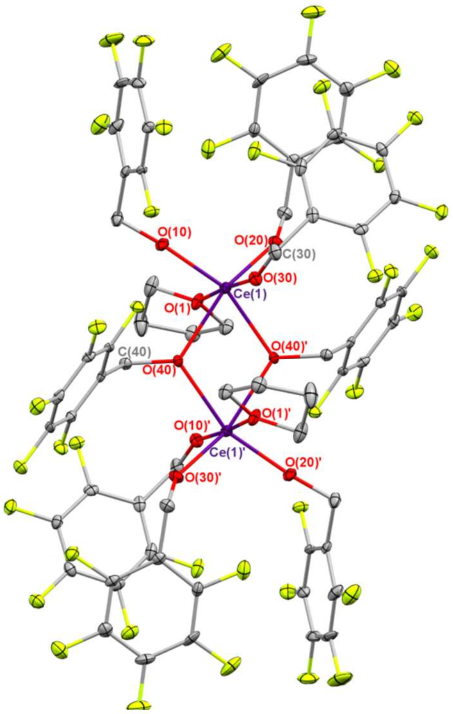

Figure 3. 30% probability thermal ellipsoid plots of **6** (top) and **7** (bottom). Hydrogen atoms have been omitted for clarity. Selected bond lengths and angles for **6**: Ce(1)–O(1): 2.3514(19) Å, Ce(1)–O(2): 2.0743(19) Å, Ce(1)–O(1)': 2.3934(18) Å, O(4)–C(37): 1.411(3) Å, O(1)–C(1): 1.423(4) Å, Ce(1)–O(1)–Ce(1)': 110.97(8)°, O(1)–Ce(1)–O(1)': 69.03(8)°. Selected bond lengths and angles for **7**: Ce(1)–O(20): 2.073(2) Å, Ce(1)–O(40): 2.385(2) Å, Ce(1)–O(40)': 2.339(2) Å, O(30)–C(30): 1.397(4) Å, O(40)–C(40): 1.416(4) Å, Ce(1)–O(40)–Ce(1)': 111.38(8)°, O(40)–Ce(1)–O(40)': 68.62(8)°.

Reaction of $Ce[N(SiHMe_2)_2]_4$ with four equivalents of $HOCH_2Ar$ (Ar = C_6Me_5, C_6F_5) in THF gave the yellow tetravalent complexes $\{Ce[OCH_2C_6Me_5]_4(THF)\}_2$ (**6**) and $\{Ce[OCH_2C_6F_5]_4(THF)\}_2$ (**7**), respectively (Scheme 2). Both **6** and **7** crystallized as dimers in the triclinic space group P-1 but were not isomorphous (Figure 3). Each complex included two benzyloxy bridging ligands that interacted with the cerium(IV) centers symmetrically (**6**, 2.3514(19) Å); **7**, 2.385(2) Å). The terminal Ce–O distances in **6** (2.0743(19)–2.1081(18) Å) were not significantly longer than in **7** (2.073(2)–2.111(2) Å), indicating that the Ce–O bond distances were not strongly influenced by the identity of the phenyl substituents. For comparison, the terminal Ce–O distances in compounds **4** (2.0897(12)–2.1203(12) Å) and **5** (2.101(3)–2.125(3) Å) were slightly longer, which reflected the increased steric demand of the ligand environments of **4** and **5** compared to **6** and **7**. A variable temperature ^1H NMR study of $\{Ce[OCH_2C_6Me_5]_4(THF)\}_2$ (**6**) showed decoalescense of the methylene and methyl resonances at –60 °C, however, the resulting, broadened signals could not easily be assigned at the low temperature limit of the experiment (–80 °C) (Figure S10). Previously reported alkoxide-bridged dicerium(IV) complexes include homoleptic $[Ce(OCMe_2{}^iPr)_4]_2$[55] and $[Ce(OCMe_3)_4]_2$,[65] proligand-coordinated $[Ce(O^iPr)_4(HO^iPr)]_2$ [66, 67] and heteroleptic $(^tBu_3CO)_3CeOC_6H_4OCe(OC^tBu_3)_3$,[68] $[Ce(O^iPr)_3(OC_2H_4NMeC_2H_4NMe_2)]_2$,[69] and $[Ce_2(dmop)_4(mmp)_2(O)]$ (dmop = 2-(4,4-dimethyl-4,5-dihydrooxazol-2-yl)propan-2-ol, mmp = 1-methoxy-2-methylpropan-2-ol).[70]

Characterization of Mononuclear Cerium(IV) Compounds

Upon isolation of compounds **3**, **4**, **5**, **6**, and **7**, it was clear that the compounds exhibited different properties based on the physical appearance of their crystalline solids and solutions. Compound **3** was dark red, compounds **4**, **6**, and **7** were yellow, and compound **5** was dark blue. These observations prompted us to explore physical characterization in order to compare the different metal-ligand interactions in these coordination environments. In this analysis, only the monomeric compounds **3**, **4**, and **5** were considered in order to provide a direct comparison between the effects of the amide, alkoxide, and aryloxide ligand fields on the cerium(IV) cation.

Broad features observed in the UV/visible region of the electronic absorption spectra of cerium(IV) coordination compounds were assigned as ligand-to-metal charge transfer transitions.[4, 6-9, 30, 31] Consistent with expectations, the electronic absorption spectra of **3**, **4**, and **5** collected in toluene (Figure 4) revealed broad transitions in the UV/Visible region. Analysis of compound **3** revealed three peaks centered at 343, 440, and 524 nm with molar absorptivities of 2980, 4550, and 959 $M^{-1}cm^{-1}$, respectively. The spectrum of compound **4** showed a maximum at 305 nm (7240 $M^{-1}cm^{-1}$). Compound **5** showed LMCT transitions at 366, 487, and 624 nm (1600, 2100, and 3380 $M^{-1}cm^{-1}$, respectively) as well as a transition at 303 nm (17200 $M^{-1}cm^{-1}$), tentatively assigned to an inter-arene charge transfer transition from the electron rich phenyl substitutents to phenoxide aromatic systems on neighboring ligands (Figure S2).[71]

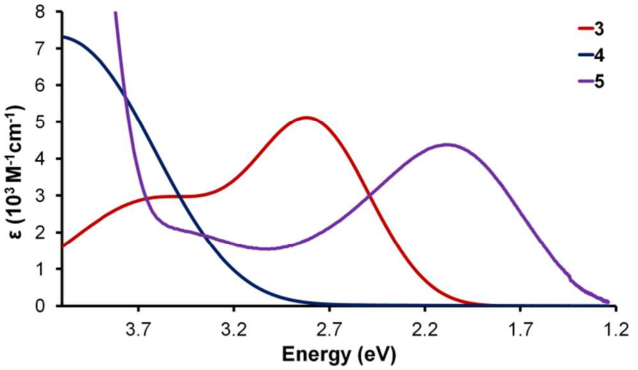

Figure 4. Electronic absorption spectra of **3**, **4**, and **5** collected in toluene.

Electrochemical data for cerium compounds with silylamide, aryloxide, and alkoxide ligand environments have been reported. However, the lack of consistency between the coordination numbers of anionic ligands in these complexes complicates an assessment of the effects of these ligand types. Cerium(III/IV) couples have been reported for compounds in tris(amido) environments: $Ce[N(SiMe_3)_2]_3$ (+0.35 V), $CeF[N(SiMe_3)_2]_3$ (–0.56 V) and $CeCl[N(SiMe_3)_2]_3$ (–0.30 V).[6, 9] Previously characterized cerium(III) aryloxide compounds were described as mild reductants ($\Delta E_{1/2}$ = –0.5 to –1.5 V versus Fc/Fc^+).[6-8, 28] The highly reducing ability of the cerium(III) ion in the presence of alkoxide ligands was previously observed in a ferrocene based ancillary ligand environment.[5]

In order to rationally describe the effects of the ligand environment on the stability of the cerium(IV) ion, electrochemical analysis was performed on compounds **3**, **4**, and **5**. Electrochemical data was collected in dichloromethane (DCM) with 0.1 M $[^nPr_4N][BAr^F_4]$. The cyclic voltammogram of compound **3** showed a quasi-reversible metal based feature centered at –1.04 V versus Fc/Fc^+ with a wave separation of 0.21 V (Figure 5). This feature was shifted to a more reducing potential compared to the cerium(III/IV) couples in related tris(amido) compounds due to the tetrakis(amido) coordination environment of **3**.[6, 9] The cyclic voltammogram of compound **4** showed a metal based reduction feature at E_{pc} = –1.99 V and a related metal based oxidation feature at E_{pa} = –1.32 V versus Fc/Fc^+. The cyclic voltammogram of compound **5** showed a reversible metal based feature centered at –0.50 V versus Fc/Fc^+ with a wave separation of 0.07 V (Figure 5). Based on this analysis, the tetrakis coordination of silylamide ligands offered intermediate thermodynamic stabilization to the cerium(IV) ion compared to the tetrakis coordination of alkoxide or aryloxide ligands. As seen in Figure 4, the more sterically restricted coordination environments in compounds **3** and **5** compared to compound **4** resulted in more reversible electrochemical features. The sterically demanding ligand environments in **3** and **5** evidently reduced the reorganization energy upon heterogeneous electron transfer and led to diminished overpotentials.[6, 28, 72]

	E (nm) / ε ($M^{-1}cm^{-1}$)	E_{pa} (V vs Fc/Fc^+)	E_{pc} (V vs Fc/Fc^+)	ΔE (V)	HOMO–LUMO (eV)	q_{Ce}
3	343 / 2980 440 / 4550 524 / 959	–0.93	–1.14	0.21	3.16	1.856
4	305 / 7240	–1.32	–1.99	0.67	4.16	1.922
5	303 / 17200 366 / 1600 487 / 2100 624 / 3380	–0.46	–0.54	0.07	2.41	1.986

Table 1. Electronic absorption, electrochemical, and computational data for **3**, **4**, and **5**.

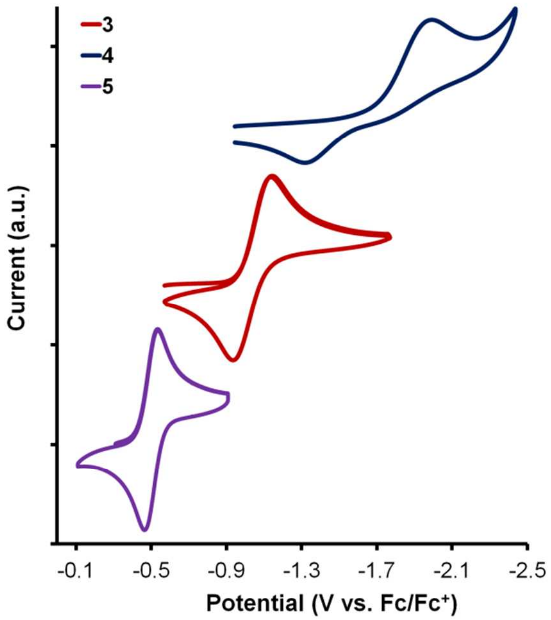

Figure 5. Isolated cerium(III/IV) redox couple in the cyclic voltammograms of **3**, **4**, and **5** collected in DCM with 0.1 M $[^{n}\mathrm{Pr}_4\mathrm{N}][\mathrm{BAr^F}_4]$; [analyte] = ca. 1 mM; v = 0.1 V/sec.

Electronic Structure of Cerium(IV) Compounds

Electronic structure calculations of compounds **3**, **4**, and **5** were performed using Gaussian '09 at the B3LYP level of theory to describe the nature of the bonding between cerium and the anionic ligands. The geometry optimized gas phase structures were found to be in excellent agreement with the crystallographically determined bond lengths and bond angles. The calculated LUMO–LUMO+6 in compounds **3**, **4**, and **5** were primarily cerium 4f in character and had minimal interactions with ligand based atomic orbitals. The HOMO–LUMO energy gaps in **3**, **4**, and **5** were 3.16, 4.16, and 2.41 eV, respectively. The increase in the calculated HOMO–LUMO energy gaps (**5** < **3** < **4**) correlated with the observed trend in the LMCT transitions in the electronic absorption spectra shown in Figure 4.

The highest occupied molecular orbitals in compound **3** were largely composed of contributions from the bis(dimethylsilyl)amido ligand atomic orbitals and showed some overlap with cerium atomic orbitals. Interactions between the cerium ion and the amido ligands in the π orientation were observed in the HOMO to HOMO–3 molecular orbitals. Interactions between the cerium ion and the amido ligands along the bonding axes were observed in the HOMO–4 to HOMO–7 molecular orbitals. Visual representations of the HOMO and HOMO–4 molecular orbitals in **3** are shown in Figure 5.

The highest occupied molecular orbitals in compound **4** were largely composed of contributions from the *tert*-butoxy ligand atomic orbitals, and showed some overlap with cerium atomic orbitals. In particular the HOMO–1 to HOMO–3 and HOMO–6 to HOMO–7 showed π interactions between the alkoxy ligands and the cerium ion. No notable interactions along the Ce–O bonding axes were apparent in the calculated molecular orbitals of compound **4**.

The highest occupied molecular orbitals in compound **5** were also largely ligand based. However, the HOMO and HOMO–1 molecular orbitals did show π interactions between the aryloxy ligands and the cerium ion. As in compound **4**, none of the calculated molecular orbitals in compound **5** showed interactions along the Ce–O bonding axes.

Natural population analysis was used to calculate the natural charges present on the component atoms in each compound. The natural charges of the cerium ions, q_{Ce}, in **3**, **4**, and **5** of 1.856, 1.922, and 1.986, respectively, indicated a higher degree of ionicity of the metal-ligand bonding in compounds **4** and **5** compared to compound **3**. Based on the comparison of this metric with the electrochemical data, no correlation between the degree of metal-ligand bond ionicity and the thermodynamic stability of the cerium(IV) center was observed.

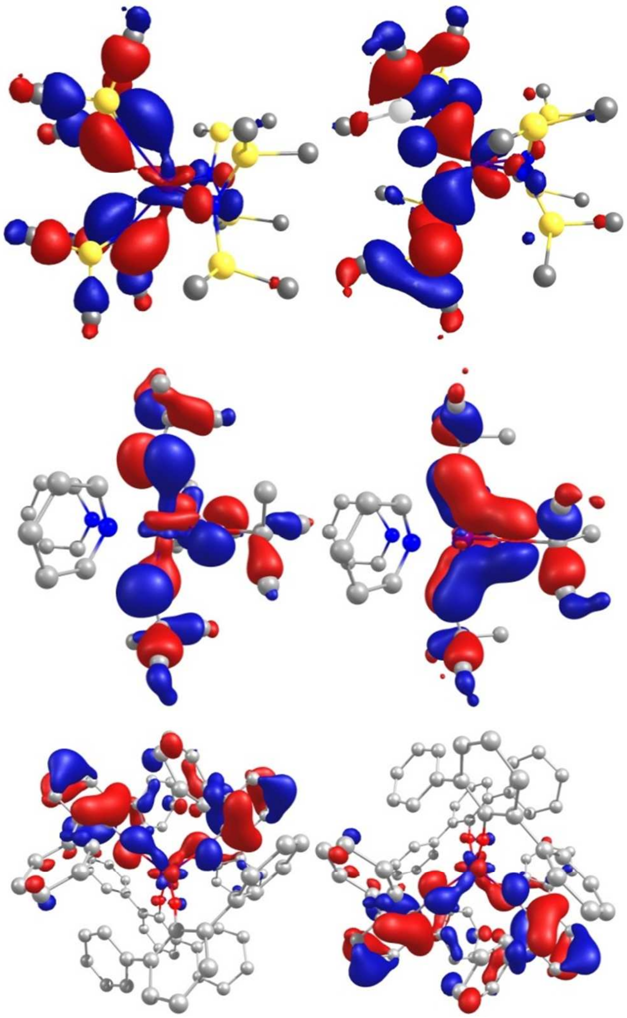

Figure 6. Top: The HOMO (left) and HOMO–4 (right) calculated molecular orbitals in **3**. Middle: The HOMO-1 (left) and HOMO-7 (right) calculated molecular orbitals in **4**. Bottom: The HOMO (left) and HOMO-1 (right) calculated molecular orbitals in **5**.

Conclusions

We oxidized $K[Ce[N(SiHMe_2)_2]_4]$ in order to isolate $Ce[N(SiHMe_2)_2]_4$ by an improved procedure. $Ce[N(SiHMe_2)_2]_4$ underwent protonolysis with *tert*-butanol, 2,6-diphenylphenol, and substituted benzyl alcohols to yield Ce(O^{t}Bu)$_4$(py)$_2$, Ce(Odpp)$_4$, and Ce$_2$(OCH$_2$C$_6$R$_5$)$_8$(THF)$_2$ (R = Me, F). Physical characterization of the monomeric cerium(IV) compounds was explored. Electronic absorption spectroscopy of the amide, alkoxide, and aryloxide complexes showed highly tunable LMCT transitions depending on the ligand environment of the cerium ion. Electrochemical analysis showed that the alkoxide complex was most strongly stabilized in the cerium(IV) oxidation state and that the aryloxide complex was the least stabilized member of the series. Computational assessment of the electronic structure of these compounds showed minimal metal-ligand overlap and no correlation between the degree of ionicity of the metal-ligand bonds and the cerium(III/IV) redox potential. This work provides a basis for the future design of molecular complexes with purposefully tuned cerium(III/IV) redox potentials and charge transfer transitions.

Acknowledgements

The authors gratefully acknowledge the Chemical Sciences, Geosciences, and Biosciences Division, Office of Basic Energy Sciences, Early Career Research Program of the U.S. Department of Energy (Award (DE-SC006518) and the German Science Foundation (Grant AN 238/16-1). We also thank the University of Pennsylvania and the Research Corporation for Science Advancement (Cottrell Scholar Award to E.J.S.) for financial support and the NSF for support of the X-ray diffractometer (Grant CHE-0840438). This work used the Extreme Science and Engineering Discovery Environment, which is supported by the U.S. National Science Foundation (Grant OCI-1053575).

Notes and references

[a] P. Roy and Diana T. Vagelos Laboratories, Department of Chemistry, University of Pennsylania, 231 South 34th Street, Philadelphia, Pennsylvania 19104, United States. E-mail: schelter@sas.upenn.edu.
[b] Institute of Inorganic Chemistry, Eberhard Karls Universität Tübingen, Auf der Morgenstelle 18, D-72076 Tübingen, Germany, Fax: (+49) 7071 29 35271, E-mail: reiner.anwander@uni-tuebingen.

Electronic Supplementary Information (ESI) available: crystallographic data, ^{1}H, ^{13}C, and ^{19}F NMR data, electronic absorption spectra, electrochemical data, computational data. CCDC: 1000019 (**2**), 1000020 (**4**), 1000021 (**5**), 1000023 (**6**), 1000022 (**7**). See DOI: 10.1039/b000000x/

1. G.-C. Wang, H. H. Y. Sung, I. D. Williams and W.-H. Leung, *Inorg. Chem.*, 2012, **51**, 3640-3647.
2. A. R. Crozier, C. Schadle, C. Maichle-Mossmer, K. W. Törnroos and R. Anwander, *Dalton Trans.*, 2013, **42**, 5491-5499.
3. U. J. Williams, B. D. Mahoney, A. J. Lewis, P. T. DeGregorio, P. J. Carroll and E. J. Schelter, *Inorg. Chem.*, 2013, **52**, 4142-4144.
4. J. A. Bogart, A. J. Lewis, S. A. Medling, N. A. Piro, P. J. Carroll, C. H. Booth and E. J. Schelter, *Inorg. Chem.*, 2013, **52**, 11600-11607.
5. E. M. Broderick, P. S. Thuy-Boun, N. Guo, C. S. Vogel, J. Sutter, J. T. Miller, K. Meyer and P. L. Diaconescu, *Inorg. Chem.*, 2011, **50**, 2870-2877.
6. J. R. Robinson, P. J. Carroll, P. J. Walsh and E. J. Schelter, *Angew. Chem. Int. Ed.*, 2012, **51**, 10159-10163.
7. B. D. Mahoney, N. A. Piro, P. J. Carroll and E. J. Schelter, *Inorg. Chem.*, 2013, **52**, 5970-5977.
8. J. R. Robinson, Z. Gordon, C. H. Booth, P. J. Carroll, P. J. Walsh and E. J. Schelter, *J. Am. Chem. Soc.*, 2013, **135**, 19016-19024.
9. U. J. Williams, J. R. Robinson, A. J. Lewis, P. J. Carroll, P. J. Walsh and E. J. Schelter, *Inorg. Chem.*, 2014, **53**, 27-29.
10. Y.-M. So, G.-C. Wang, Y. Li, H. H. Y. Sung, I. D. Williams, Z. Lin and W.-H. Leung, *Angew. Chem. Int. Ed.*, 2014, **53**, 1626-1629.
11. T. Behrsing, A. M. Bond, G. B. Deacon, C. M. Forsyth, M. Forsyth, K. J. Kamble, B. W. Skelton and A. H. White, *Inorg. Chim. Acta*, 2003, **352**, 229-237.
12. P. B. Hitchcock, M. F. Lappert and A. V. Protchenko, *Chem. Commun.*, 2006, 3546-3548.
13. A. R. Crozier, A. M. Bienfait, C. Maichle-Mossmer, K. W. Törnroos and R. Anwander, *Chem. Commun.*, 2013, **49**, 87-89.
14. P. L. Arnold, I. J. Casely, S. Zlatogorsky and C. Wilson, *Helv. Chim. Acta*, 2009, **92**, 2291-2303.
15. W. J. Evans, T. J. Deming, J. M. Olofson and J. W. Ziller, *Inorg. Chem.*, 1989, **28**, 4027-4034.
16. W. J. Evans, T. J. Deming and J. W. Ziller, *Organometallics*, 1989, **8,** 1581-1583.
17. P. Dröse, J. Gottfriedsen, Cristian G. Hrib, Peter G. Jones, L. Hilfert and Frank T. Edelmann, *Z. Anorg. Allg. Chem.*, 2011, **637**, 369-373.
18. L. G. Hubert-Pfalzgraf, V. Abada and J. Vaissermann, *J. Chem. Soc. Dalton Trans.*, 1998, 3437-3442.
19. F. Ribot, P. Toledano and C. Sanchez, *Chem. Mater.*, 1991, **3**, 759-764.
20. D. Werner, G. B. Deacon, P. Junk, C. and R. Anwander, *Chem. Eur. J.*, *2014* **20,** 4426-4438.
21. W. A. Herrmann, R. Anwander, F. C. Munck, W. Scherer, V. Dufaud, N. W. Huber and G. R. J. Artus, *Z. Naturforsch.* 1994, **49B**, 1789-1797.
22. O. Runte, T. Priermeier and R. Anwander, *Chem. Commun.*, 1996, 1385-1386.
23. R. Anwander, J. Eppinger, I. Nagl, W. Scherer and M. Tafipolsky, *Inorg. Chem.*, 2000, **39**, 4713-4720.
24. F. Estler, E. Herdtweck and R. Anwander, *J. Chem. Soc., Dalton Trans.*, 2002, 3088-3089.
25. C. Meermann, P. Sirsch, K. W. Törnroos and R. Anwander, *Dalton Trans.*, 2006, 1041-1050.
26. Q. Liu, C. Meermann, H. W. Gˆrlitzer, O. Runte, E. Herdtweck, P. Sirsch, K. W. Törnroos and R. Anwander, *Dalton Trans.*, 2008, 6170–6178.
27. C. Meermann, K. W. Törnroos and R. Anwander, *Inorg. Chem.*, 2009, **48**, 2561–2570.
28. N. A. Piro, J. R. Robinson, P. J. Walsh and E. J. Schelter, *Coord. Chem. Rev.*, 2014, **260**, 21-36.
29. G. F. Smith and C. A. Getz, *Ind. Eng. Chem., Anal. Ed.*, 1938, **10**, 191-195.
30. J. R. Robinson, C. H. Booth, P. J. Carroll, P. J. Walsh and E. J. Schelter, *Chem. – Eur. J.*, 2013, **19**, 5996-6004.
31. A. Vogler and H. Kunkely, *Inorg. Chim. Acta*, 2006, **359**, 4130-4138.
32. M. Wojdyr, *J. Appl. Crystallogr.*, 2010, **43**, 1126-1128.
33. Bruker, *SMART, SAINT, SADABS and XPREP. Area detector control and data integration and reduction software,* Bruker AXS, Inc., Madison, WI, USA, 2008.
34. G. Sheldrick, *Acta Crystallogr. Sect. A*, 2008, **64**, 112-122.

35. M. J. Frisch, G. W. Trucks, H. B. Schlegel, G. E. Scuseria, M. A. Robb, J. R. Cheeseman, G. Scalmani, V. Barone, B. Mennucci, G. A. Petersson, H. Nakatsuji, M. Caricato, X. Li, H. P. Hratchian, A. F. Izmaylov, J. Bloino, G. Zheng, J. L. Sonnenberg, M. Hada, M. Ehara, K. Toyota, R. Fukuda, J. Hasegawa, M. Ishida, T. Nakajima, Y. Honda, O. Kitao, H. Nakai, T. Vreven, J. Montgomery, J. A., J. E. Peralta, F. Ogliaro, M. Bearpark, J. J. Heyd, E. Brothers, K. N. Kudin, V. N. Staroverov, R. Kobayashi, J. Normand, K. Raghavachari, A. Rendell, J. C. Burant, S. S. Iyengar, J. Tomasi, M. Cossi, N. Rega, J. M. Millam, M. Klene, J. E. Knox, J. B. Cross, V. Bakken, C. Adamo, J. Jaramillo, R. Gomperts, R. E. Stratmann, O. Yazyev, A. J. Austin, R. Cammi, C. Pomelli, J. W. Ochterski, R. L. Martin, K. Morokuma, V. G. Zakrzewski, G. A. Voth, P. Salvador, J. J. Dannenberg, S. Dapprich, A. D. Daniels, Ö. Farkas, J. B. Foresman, J. V. Ortiz, J. Cioslowski and D. J. Fox, Gaussian 09, Revision A.02, Gaussian, Inc., Wallingford CT, 2009.
36. M. Dolg, H. Stoll and H. Preuss, *J. Chem. Phys.*, 1989, **90**, 1730-1734.
37. G. A. Zhurko and D. A. Zhurko, http://chemcraftprog.com/.
38. D. C. Bradley, J. S. Ghotra and F. A. Hart, *J. Chem. Soc., Dalton Trans.*, 1973, 1021-1023.
39. R. Anwander, O. Runte, J. Eppinger, G. Gerstberger, E. Herdtweck and M. Spiegler, *J. Chem. Soc., Dalton Trans.*, 1998, 847-858.
40. A. R. Smith and T. Livinghouse, *Organometallics*, 2012, **32**, 1528-1530.
41. S. M. Mansell, B. F. Perandones and P. L. Arnold, *J. Organomet. Chem.*, 2010, **695**, 2814-2821.
42. R. K. Thomson, B. L. Scott, D. E. Morris and J. L. Kiplinger, *C. R. Chim.*, 2010, **13**, 790-802.
43. G. W. Rabe and G. P. A. Yap, *Z. Krist.-New Cryst. Struct.*, 2000, **215**, 457-458.
44. M. Rastätter, A. Zulys and P. W. Roesky, *Chem. – Eur. J.*, 2007, **13**, 3606-3616.
45. B. Saha, M.-H. Lin and T. V. RajanBabu, *J. Org. Chem.*, 2007, **72**, 8648-8655.
46. G. Occhipinti, C. Meermann, H. M. Dietrich, R. Litlabø, F. Auras, K. W. Törnroos, C. Maichle-Mössmer, V. R. Jensen and R. Anwander, *J. Am. Chem. Soc.*, 2011, **133**, 6323-6337.
47. H. Skår, J. G. Seland, Y. Liang, N. Å. Frøystein, K. W. Törnroos and R. Anwander, *Eur. J. Inorg. Chem.*, 2013, 5969-5979.
48. D. Bubrin and M. Niemeyer, *Inorg. Chem.*, 2014, **53**, 1269-1271.
49. D. Schneider, D. Werner, C. Maichle-Mössmer, P. Junk, G. B. Deacon and R. Anwander, presented in part at the Terrae Rarae, Stuttgart, Germany, 2013.
50. L. Yang, D. R. Powell and R. P. Houser, *Dalton Trans.*, 2007, 955-964.
51. C. Meermann, G. Gerstberger, M. Spiegler, K. W. Törnroos and R. Anwander, *Eur J. Inorg. Chem.*, 2008, 2014-2023.
52. J. Schläfer, S. Stucky, W. Tyrra and S. Mathur, *Inorg. Chem.*, 2013, **52**, 4002-4010.
53. D. L. Clark and J. G. Watkin, *Inorg. Chem.*, 1993, **32**, 1766-1772.
54. S. Daniele, L. G. Hubert-Pfalzgraf and M. Perrin, *Polyhedron*, 2002, **21**, 1985-1990.
55. S. Suh, J. Guan, L. A. Miinea, J.-S. M. Lehn and D. M. Hoffman, *Chem. Mater.*, 2004, **16**, 1667-1673.
56. G. B. Deacon, T. Feng, P. C. Junk, B. W. Skelton and A. H. White, *J. Chem. Soc., Dalton Trans.*, 1997, 1181-1187.
57. G. B. Deacon, C.- M- Forsyth, P. C. Junk, B. W. Skelton and A. H. White, *Chem. Eur. J.*, 1999, **5**, 1452-1459.
58. G. B. Deacon, P. D. Junk, G. J. Moxey, K. Ruhlandt-Senge, C. St Prix and M. F. Zuniga, *Chem. Eur. J.*, 2009, **15**, 5503-5519.
59. G. B. Deacon, P. D. Junk, G. J. Moxey and J. Graeme, *Chem. Asian J.*, 2009, **4**, 1309-1317.
60. D. L. Clark, G. B. Deacon, T. Feng, R. V. Hollis, B. L. Scott, B. W. Skelton, J. G. Watkin and A. H. White, *Chem. Commun.*, 1996, 1729-1730.
61. G. B. Deacon, A. Gitlits, P. C. Junk, B. W. Skelton and A. H. White, *Z. Anorg. Allg. Chem.*, 2005, **631**, 861-865.
62. Y. Yao, X. Xu, B. Liu, Y. Zhang, Q. Shen and W.-T. Wong, *Inorg. Chem.*, 2005, **44**, 5133-5140.
63. K. Nie, W. Gu, Y. Yao, Y. Zhang and Q. Shen, *Organometallics*, 2013, **32**, 2608-2617.
64. K. Nie, L. Fang, Y. Yao, Y. Zhang, Q. Shen and Y. Wang, *Inorg. Chem.*, 2012, **51**, 11133-11143.
65. J. Schläfer, W. Tyrra and S. Mathur, *Inorg. Chem.*, 2014, **53**, 2751-2753.
66. P. P. Toledano, F. Ribot, C. Sanchez, *Acta Cryst. C*, 1990, **46**, 1419-1422.
67. B. A. Vaartstra, J. C. Huffmann, P. S. Gradeff, L. G. Hubert-Pfalzgraf, J.-C. Daran, S. Parraud, K. Yunlu, K. G. Caulton, *Inorg. Chem.*, 1990, **29**, 3126-3131.
68. A. Sen and H. A. Stecher, A. L. Rheingold, *Inorg. Chem.*, 1992, **31**, 473-479.
69. L. G. Hubert-Pfalzgraf, N. El Khokh and J.-C. Daran, *Polyhedron*, 1992, **11**, 59-63.
70. H. C. Aspinall, J. Basca, A. C. Jones, J. S. Wrench, K. Black, P. R. Chalker, P. J. King, P. Marshall, M. Werner, H. O. Davies and R. Odedra, *Inorg. Chem.*, 2011, **50**, 11644-11652.
71. A. Acosta, J. I. Zink and J. Cheon, *Inorg. Chem.*, 2000, **39**, 427-432.
72. I. J. Casely, S. T. Liddle, A. J. Blake, C. Wilson and P. L. Arnold, *Chem. Commun.*, 2007, 5037-5039.

Abstract:

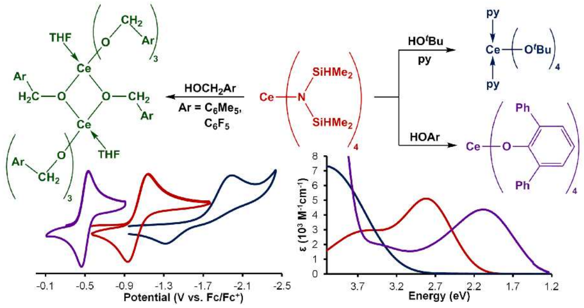

New cerium(IV) compounds, isolated by the reaction of Ce[N(SiHMe$_2$)$_2$]$_4$ with alcohols and phenols, exhibited variable electronic transitions and reduction potentials.